4th International Symposium on Geotechnical Engineering
for the Preservation of Monuments and Historic Sites

ID. TC301-2026-58

A Simplified 2D Methodology for Assessing the Stability of Carved Mycenaean Tombs Under Asymmetrical Geological Conditions

D. Egglezos [1], L. Pantelidis[2]

[1]Phd Civil Engineer, GEOPER SA, Hellenic Open University (HoU), dimitrios.egglezos@gmail.com

[2]Phd, Associate Professor of Civil Engineering, Department of Civil Engineering and Geomatics

Cyprus University of Technology (CUT), lysandros.pantelidis@cut.ac.cy

ABSTRACT

Rock-carved Mycenaean chamber tombs often exhibit complex geological asymmetry, such as stratification, discontinuities, weathering, and nearby slopes, while their structural response is inherently three-dimensional. In fully closed chambers, excavation induces circumferential (hoop) stresses along horizontal rings of the cavity, generating a ring-type confinement mechanism that significantly enhances stability. This mechanism is captured by axisymmetric analysis but is entirely absent in plane-strain models, which are nevertheless required to represent real-world asymmetry. As a result, direct plane-strain modelling of ring-type chambers can systematically exaggerate deformation and yielded zones and may lead to unnecessarily heavy or poorly targeted interventions. This paper proposes a simplified hybrid ("pseudo-3D") methodology that restores the missing confinement in a 2D asymmetric model through an equivalent stabilizing pressure profile $\mathrm{p_n(z)}$.The confinement function is derived analytically using Kirsch-type elastic solutions and/or extracted from staged axisymmetric reference analyses, and is then introduced into a plane-strain model that includes the actual stratigraphy and boundary conditions. The method is presented for both fully closed and fully open roof configurations (with brief reference to intermediate cases), and is illustrated through an exemplary application for the carved tomb T1 at Pellana.

Keywords: Carved Mycenaean tombs; pseudo-3D stability; hoop stresses; confinement correction; Kirsch solution; axisymmetric reference; plane strain; cultural heritage conservation.

INTRODUCTION

Rock-carved Mycenaean chamber tombs constitute a distinctive class of underground monuments whose stability depends on the geometry of excavation and the mechanical behavior of the surrounding rock mass. Many have experienced roof degradation and partial collapse over time, resulting in current geometries that differ substantially from their original, fully enclosed form (see Figure 1, left). Stability and conservation decisions require engineering assessment methods that are mechanically consistent but also practical for monument-scale applications.

For closed and embedded cavities of approximately rotational geometry (see Figure 1, right), excavation induces a three-dimensional circumferential stress field around horizontal rings of the opening. This "ring action" generates confinement and contributes significantly to stability. Such axisymmetric analysis captures this mechanism naturally, whereas plane-strain modelling suppresses the circumferential direction and therefore the associated confinement. Plane strain is, however, required to represent the geological and boundary-condition asymmetries that control many real sites (dipping stratigraphy, joints, slopes, surface loads). Consequently, a direct plane-strain model of a ring-type chamber may predict excessive deformation and plasticity and yield over-conservative and potentially misleading support demands.
This paper proposes a simplified hybrid ("pseudo-3D") methodology. A confinement function $p_n(z)$ is derived from axisymmetric reference analyses and/or Kirsch-type analytical relations and is then

introduced into the plane-strain asymmetric model as an equivalent stabilizing pressure varying with depth. The objective is to recover the essential stabilizing mechanism of hoop confinement while preserving the ability of the plane-strain model to represent actual site asymmetry.

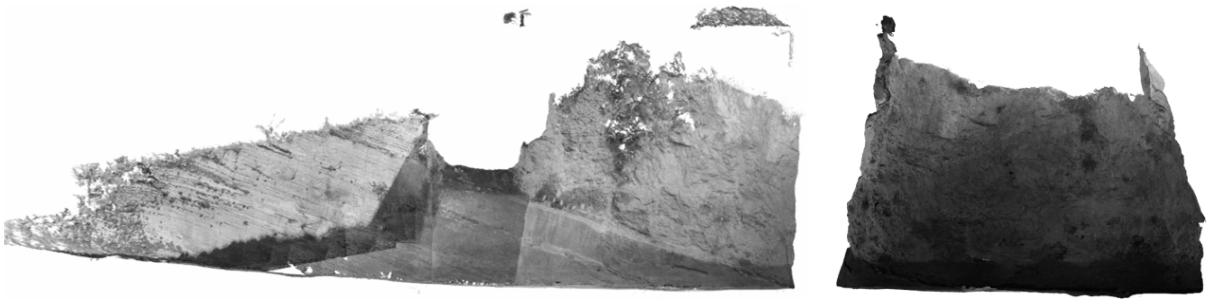

Figure 1. *Left: Longitudinal section along the "Dromos" of Mycenaean Tomb 1 at the Pellana archaeological site; Right: Transverse section of Mycenaean Tomb 1 at the Pellana archaeological site, perpendicular to the longitudinal section (Orestidis D., 2022).*

GEOMETRY AND STRUCTURAL IDEALIZATION OF CARVED CONOIDAL TOMBS

Many carved Mycenaean chamber tombs can be idealized, at a first-order mechanical level, as approximately rotational cavities with conoidal or spheroidal profiles (Figure 2). The chamber geometry is described through the radius of the cavity boundary as a function of depth, denoted $R(z)$, where z denotes the vertical coordinate. Depth z is measured downward from an adopted reference datum corresponding to the initial ground surface ($z = 0$). For the representation of the excavation history and subsequent degradation, three characteristic elevation levels are defined: $z_0 = 0$, corresponding to the initial surface; z_c, denoting the crown level of the originally closed roof; and z_{co}, representing the crown level of the present configuration after roof collapse or erosion. A fully open roof condition corresponds to complete removal of the roof and overburden above z_{co}, whereas partially open roofs correspond to intermediate stages of degradation, briefly discussed in the following sections.

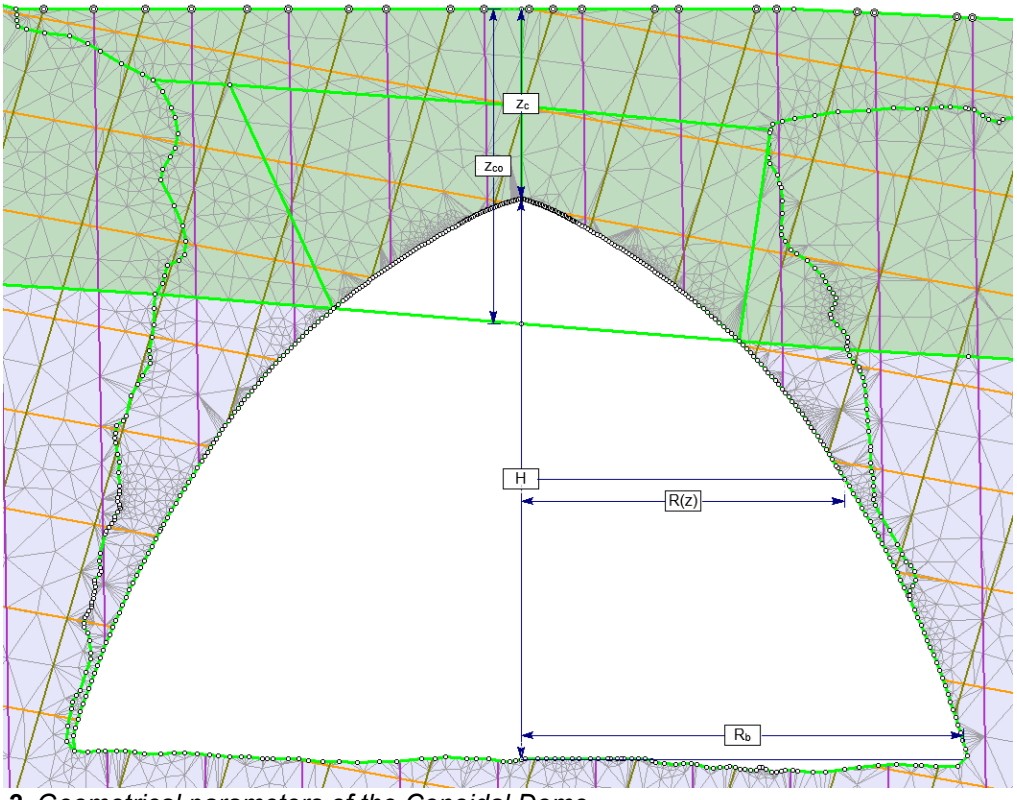

Figure 2. *Geometrical parameters of the Conoidal Dome*

THEORETICAL EVALUATION OF 2-D ANALYSES FOR CARVED MYCENAEAN-TYPE TOMBS

Plane-strain models are essential for capturing real geological asymmetries—such as stratification, discontinuities, slopes, and local loads—but they suppress the circumferential direction and cannot mobilize ring-type confinement. This often leads to exaggerated displacements and plastic zones near the cavity.

In contrast, axisymmetric analyses naturally capture hoop stresses and are well suited for rotational cavities, especially in their original closed-roof form. However, they cannot represent asymmetric geology or boundary conditions and are therefore insufficient on their own.

To reconcile these limitations, a hybrid pseudo-3D approach is adopted. The depth-dependent confinement pressure $p_n(z)$ is derived from axisymmetric or analytical models and introduced into the plane-strain model as a stabilizing boundary load. This restores the missing hoop action while retaining the realistic geological representation.

ANALYTICAL AND NUMERICAL CALCULATION OF STABILIZING PRESSURE PROFILE $p_n(z)$.

This section describes the derivation and numerical implementation of the depth-dependent stabilizing pressure $p_n(z)$, which represents the hoop confinement mobilized around ring-type cavities.

Let θ denote the circumferential direction about the axis of symmetry, with corresponding normal stress σ_θ(the hoop stress). The angle ϕ defines the location along the cavity boundary in the meridional (r–z) plane. The cavity boundary at elevation $z$has radius $R(z)$, and the vertical coordinate $z$is measured downward from the initial ground surface ($z = 0$).

At each elevation z, the horizontal ring defined by the cavity boundary of radius $R(z)$is locally approximated as a circular opening excavated in a homogeneous elastic medium. Under general far-field in-plane stresses $\sigma_x(z)$, $\sigma_y(z)$, shear stress $\tau_{xy}(z)$, and a radial boundary traction $t_r(z)$acting on the cavity wall (compression taken as positive), the hoop stress at the cavity boundary is given by the classical Kirsch solution (Kirsch, 1898; Timoshenko & Goodier, 1970):

$$\sigma_\theta(R(z), z; \varphi) = \sigma_x(z) + \sigma_y(z) - 2\left[\sigma_x(z) - \sigma_y(z)\right]\cos(2\varphi) - 4\,\tau_{xy}(z)\,sin(2\varphi) - t_r(z) \quad (1)$$

Under gravity-dominated conditions ($\tau_{xy}(z) = 0$, $t_r(z) = 0$, $\sigma_x = \sigma_h, \sigma_y = \sigma_v$), this reduces to:

$$\sigma_\theta(R(z), z; \varphi) = \sigma_h(z) + \sigma_v(z) - 2[\sigma_h(z) - \sigma_v(z)]cos(2\phi) \quad (2)$$

The far-field hoop stress is taken as $\sigma_{\theta,\infty}(z) = \sigma_h(z) = K_0\gamma z$, where γ is the unit weight and K_0 is the at-rest lateral stress coefficient. The hoop-stress perturbation is defined as: $\Delta\sigma_\theta(r, z) = \sigma_\theta(r, z) - \sigma_h(z)$ To quantify the confinement region, a decay parameter $\kappa \in (0,1)$is introduced such that:

$$\kappa = \frac{\Delta\sigma_\theta(r_{\text{eff}}, z)}{\Delta\sigma_\theta(R, z)} \text{ with } \Delta\sigma_\theta(r, z) = \sigma_\theta(r, z) - \sigma_{\theta,\infty}(z) \quad (3)$$

Using the dominant Kirsch decay form:

$$\Delta\sigma_\theta(r, z) \approx \Delta\sigma_\theta(R(z), z)\left(\frac{R(z)}{r}\right)^2, r \geq R(z) \quad (4)$$

the following closed-form expressions are obtained:

$$r_{\text{eff}} = \frac{R(z)}{\sqrt{\kappa}},\ t_{\text{eff}}(z) = r_{\text{eff}} - R(z) = R(z)\left(\frac{1}{\sqrt{\kappa}} - 1\right), \beta(z) = \frac{t_{\text{eff}}(z)}{R(z)} = \frac{1}{\sqrt{\kappa}} - 1 \quad (5)$$

The equivalent stabilizing pressure $p_n(z)$is the average hoop-induced confinement acting radially across the effective thickness $t_{\text{eff}}(z)$:

$$p_n(z) = \frac{1}{R(z)} \int_{R(z)}^{R(z)+t_{\text{eff}}(z)} \Delta\sigma_\theta(r,z)\, dr \quad (6)$$

Using the same decay approximation, this expression reduces to

$$p_n(z) = \Delta\sigma_\theta(R(z),z)\frac{\beta(z)}{1+\beta(z)} = \Delta\sigma_\theta(R(z),z)\left(1-\sqrt{\kappa}\right) \quad (7)$$

According to the Equations 3 - 7, and under the adopted remaining-fraction definition $\kappa = \Delta\sigma_\theta(r_{eff,z})/\Delta\sigma_\theta(R,z) \in (0,1)$, *the Kirsch-type decay assumption yields* $\beta = \frac{1}{\sqrt{\kappa}} - 1$ *and* $p_n = \Delta\sigma_\theta(R,z)\cdot(1-\sqrt{\kappa})$. *For* $\Delta\sigma_\theta(R,z) > 0$, the stabilizing pressure p_n *increases monotonically as* κ *decreases, since the effective confinement zone extends further into the rock mass. Moreover, since* $\Delta\sigma_\theta(R,z)$ *depends on the far-field hoop reference* $\sigma_{\theta,\infty}(z)$ *(e.g.,* $\sigma_{\theta,\infty}(z) = K_0\cdot\gamma\cdot z$, *with* K_0 *selectable using generalized correlations such as Pantelidis, 2019), lower* K_0 *values generally increase* $\Delta\sigma_\theta(R,z)$ *and therefore increase stabilizing pressure in the embedded ring-closed portion of the chamber. These monotonic trends support transparent parameter selection and sensitivity checks without requiring full 3D modelling.*
The main geometrical and stress quantities involved in the derivation of the stabilizing pressure are illustrated in Figure 3.

The boundary stress $\sigma_\theta(R(z),z)$ can be determined analytically from Equation 2 for a selected ϕ, or numerically from an axisymmetric reference model. The same decay parameter $\kappa$is used to ensure consistency across approaches.

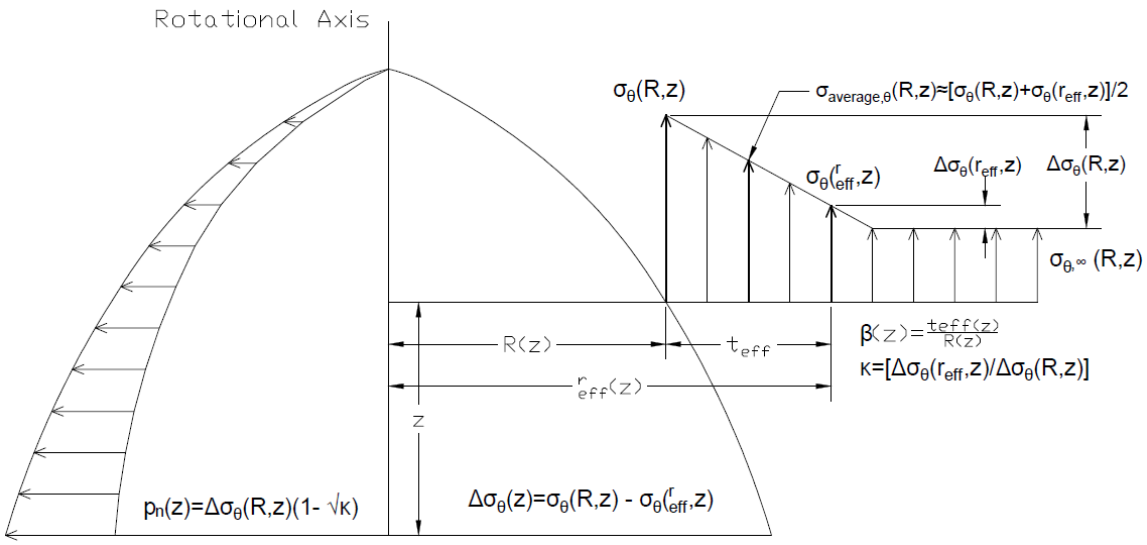

Figure 3. Geometrical and structural parameters of a Conoidal type Cavity**.**

NUMERICAL TRANSFER OF CONFINEMENT INTO PLANE-STRAIN ANALYSIS

To account for three-dimensional confinement in plane-strain models, staged axisymmetric reference analyses are conducted to quantify the hoop confinement at each stage: 1) initial geostatic stage, 2) excavation of the original chamber with closed roof, and 3) roof collapse and removal of overburden above the crown level z_c. All numerical analyses were performed using the finite-element code RS2 (Rocscience Inc., 2023).
Specifically, for each axisymmetric stage j (excavation/closed roof, weathering–cover degradation, and roof-loss/open-roof), a distinct confinement profile $p_n^j(z)$ *is extracted from the corresponding hoop-stress field and applied to the matching plane-strain stage. This one-to-one mapping preserves the staged stress path and avoids using a single* $p_n(z)$ *profile across different geometric configurations.*

From the stress profiles at each stage, $\Delta\sigma_\theta(r,z)$ is computed and used to evaluate the effective radius $r_{\text{eff}}(z)$ and the corresponding $p_n(z)$ by numerical integration:

$$p_n(z) = \frac{1}{R(z)} \int_{R(z)}^{r_{\text{eff}}(z)} \Delta\sigma_\theta(r,z)\, dr \quad (8)$$

In zones above the collapsed crown, confinement vanishes and $p_n(z) \to 0$. Below this level, confinement persists and is transferred into the 2D model.

APPLICATION IN ASYMMETRIC PLANE-STRAIN MODELLING

In the final 2D model, which accounts for realistic site asymmetry (e.g., stratigraphy, joints, slopes, local loads), the computed $p_n(z)$ is applied as a depth-dependent boundary traction along the cavity perimeter. This pseudo-3D correction restores the critical stabilizing mechanism of hoop confinement without requiring a full 3D analysis.

The rock mass strength is defined using the Hoek–Brown criterion (Hoek & Brown, 1980; Hoek et al., 2002), with parameters derived from geological and GSI-based site data. The strength characterization includes the intact uniaxial compressive strength σ_{ci}, material constant m_i, GSI index, and disturbance factor D, which are used to compute the equivalent cohesion c, friction angle ϕ, and tensile strength $\sigma_t$of the rock mass.

The main focus here is on the transfer of confinement, not on detailed strength parameter calibration.

SPECIFIC MODELLING CONSIDERATIONS

Seismic and Surface Loading Effects; Calibration Approach

In the present implementation, the confinement correction is transferred in a staged manner: the $p_n(z)$ profile used in each plane-strain stage is taken from the corresponding axisymmetric stage (closed-roof excavation, weathering/cover degradation, and roof-loss/open-roof). For pseudostatic runs, the relevant staged $p_n(z)$ profile is applied in the seismic step unless a dedicated seismic reference stage is computed; if a seismic-consistent reference profile is generated, it can be transferred in the same way.
Specifically, the confinement profile $p_n(z)$ used in pseudostatic analyses is typically taken from the relevant gravity-based reference stage, so the seismic comparison isolates the effect of inertial body forces in the asymmetric model. If a seismic-consistent confinement profile were generated, the hoop response would become azimuthally non-uniform; for design the governing sector is the reduced-confinement side, so an enveloped directional profile would be expected to yield a smaller effective $t_{eff}(z)$ (and thus smaller $p_n(z)$) than the corresponding static/gravity profile.

Surface Structures and Shelter Foundation Loads: Structures such as protective shelters are explicitly modeled in the plane-strain framework. Their effects are represented through applied surface pressures, surcharges, or foundation contact stresses. These loads are combined with the confinement correction $p_n(z)$ to simulate realistic boundary conditions under staged excavation and construction.

Calibration Philosophy: The analytical confinement model yields a closed-form relationship between the decay parameter κ and the normalized confinement width $\beta = 1/\sqrt{\kappa} - 1$. Axisymmetric numerical analyses, for a prescribed value of κ, provide direct estimates of $p_{n,n}(z)$ and the associated $\beta_n(z)$. Calibration is performed by comparing the analytical and numerical confinement pressures, $p_{n,a}(z)$and $p_{n,n}(z)$, and by assessing the alignment of the analytical $\beta(\kappa)$ with representative numerical values $\bar{\beta}_n$over the embedded portion of the chamber.
In the proposed workflow the analytical formulation serves as a rapid first estimate of the confinement correction and as an independent check on the numerical extraction. When axisymmetric reference analyses are available, the extracted $p_n(z)$ and $\beta_n(z)$ profiles are used to calibrate (and, if needed, refine) the analytical parameter κ and the resulting corresponding confinement profile. Conversely, where axisymmetric modelling is impractical, the Kirsch-based expressions provide a defensible preliminary confinement profile suitable for screening analyses.

Closed, Fully Open, and Partially Open Roof Configurations

Closed Roof: For a chamber with an intact roof and overburden, the ring confinement mechanism is fully active. The confinement pressure $p_n(z)$ is computed for the excavation stage and applied directly within the asymmetric plane-strain model.

Fully Open Roof: In configurations where the roof has collapsed down to a level z_{co}(i.e., skylight-type opening), ring confinement is largely suppressed above this level. Accordingly, $p_n(z)$approaches zero at the surface (z = 0). A practical implementation involves a linearly varying confinement pressure from $p_n(z_{co})$ at the level $z_{co}$to zero at the surface. For conservative design purposes, the pressure above z_{co}may be neglected entirely.

Partially Open Roof: When only a portion of the original roof has been lost, the resulting confinement is non-uniform around the ring. A rigorous three-dimensional treatment of this scenario is beyond the scope of the present study. Here, the issue is acknowledged and handled pragmatically, either by using staged axisymmetric reference analyses with a conservative reduction in the affected zone and/or by reserving a dedicated reduction factor for future refinement. For clarity and practical relevance, the proposed methodology and accompanying case study focus primarily on the two limiting cases: the closed roof and the fully open roof.

ILLUSTRATIVE CASE STUDY: CARVED TOMB T1 AT PELLANA (LACONIA, GREECE)

This case study demonstrates how the proposed hybrid 3D–2D methodology captures key stability mechanisms and supports the design of targeted interventions in carved chamber tombs. Tomb T1 at Pellana (Laconia, Greece) is selected as a representative example due to its conoidal geometry, partially open roof, and pronounced geological features, including stratification, discontinuities, and localized surface loading from an overhead protective shelter. The study illustrates the derivation of the confinement pressure profile $p_n(z)$ and its application in corrected plane-strain models that help distinguish true instability mechanisms from numerical artifacts.

Geometry and geological setting

The geotechnical properties of the rock mass (Geo.Per. SA, 2022) surrounding Tomb T1 are summarized in Table 1. These parameters are drawn from site investigations and laboratory testing reported in the geotechnical study by Geo.Per. SA (2022). They include intact and residual strength values, GSI estimates, and joint set orientations and spacings, and are used consistently in both axisymmetric and asymmetric analyses.

For the purposes of the numerical analyses, two complementary geostructural models were developed for Tomb T1: an asymmetric two-dimensional plane-strain model used to represent the actual stratigraphy, geometry (Orestidis D., 2022), architectural features (Orestidis G., 2022) and boundary conditions of the site, and a corresponding axisymmetric model, used as a reference framework for the quantification of circumferential confinement. The two models are shown in Figure 4.
The axisymmetric reference model is used to quantify circumferential confinement and is therefore implemented as an equivalent continuum model; discontinuities are incorporated implicitly through rock-mass properties (e.g., Hoek–Brown parameters derived from GSI and disturbance). Directional weakness associated with mapped joint sets and site-specific asymmetry is introduced in the plane-strain model, where it controls kinematics and stability.

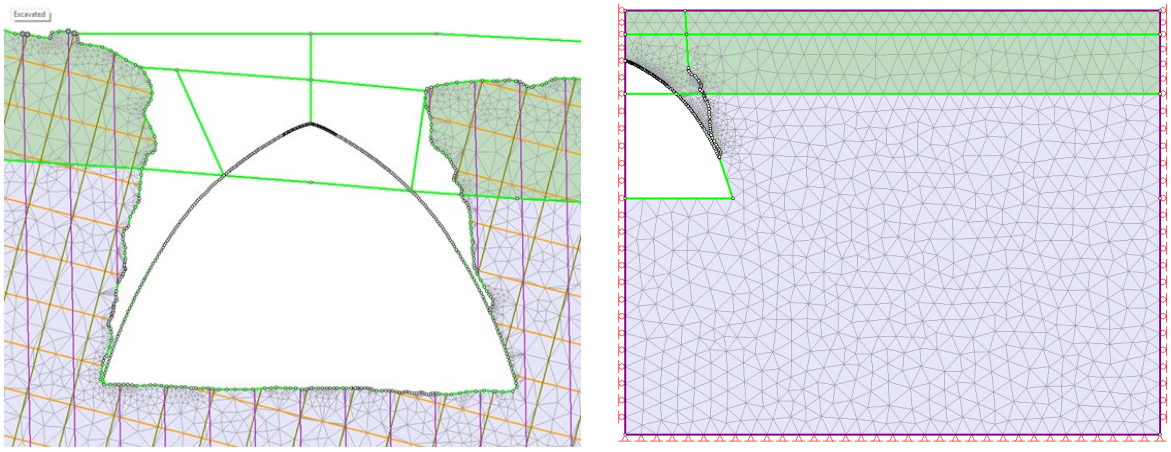

Figure 4. *Left: Geostructural model (2-D plane strain, asymmetric) of the largest Mycenaean Carved Tomb in the archaeological site of Pellana (Laconia). Right: Geostructural model (2-D axisymmetric) of the largest Mycenaean Carved Tomb in the archaeological site of Pellana (Laconia).*

Table 1. Geotechnical properties [a]

Category	Parameter	Unit	M1 (Upper Unit)	M2 (Lower Unit)
Rock mass	Unit weight, γ	kN/m³	22	24
	Young's modulus, E	kPa	258,190	941,338
	Poisson's ratio, ν	–	0.25	0.25
	Intact UCS, σ_c	kPa	15,000	15,000
	Geological Strength Index, GSI	–	*35*	55
	Strength, σci	MPa	0.361	1.207
	Geological Strength Index, GSI (Residual)	–	30	50
	Strength, σci (Residual)	MPa	0.258	0.903
Joint sets	JS1 – Dip direction / Dip / Spacing	° / ° / m	314 / 15 / 1.0	
	JS2 – Dip direction / Dip / Spacing	° / ° / m	224 / 75 / 1.0	
	JS3 – Dip direction / Dip / Spacing	° / ° / m	31 / 89 / 1.0	
Joint shear strength	Cohesion, c	kPa	110	
	Shear strength angle, φ	°	45	

[a] The geotechnical properties are drawn from the relevant geotechnical study (Geo.Per. SA, 2022)

Analytical Confinement Parameters

For the Tomb T1 application, the confinement thickness is governed by a selected remaining-fraction decay parameter, κ_{sel} = 0.40. This value expresses that the hoop-stress perturbation remains significant only within a limited radial extent from the cavity boundary, which is consistent with a jointed rock mass where circumferential stress transfer is expected to be less persistent than in intact rock. For this value, the normalized confinement thickness is $\beta_n(z) = 1/\sqrt{\kappa} - 1 = 0.581$. The corresponding stabilizing pressure is calculated analytically using the expression:

The simplified Kirsch-based framework can be extended by adopting stratum-dependent decay parameters (e.g., κ_{M1} and κ_{M2}) to reflect differences in joint persistence, spacing, and rock-mass structure. In the present contribution, a single κ value is retained for transparency and ease of application; stratigraphic effects are then reflected through the axisymmetric extraction used for calibration.

$$p_n(z) = \Delta\sigma_\theta(R, z) \cdot (1 - \sqrt{\kappa}) \quad (9)$$

Axisymmetric Reference Stages and Numerical Extraction of $p_n(z)$

A staged axisymmetric reference analysis is performed with the following sequence: 1) Initial geostatic field, 2) Excavation with intact overburden, 3) Progressive weathering of the cover soil, and 4) Final roof loss down to level z_{co}. *The confinement-extent quantities used to define the stabilizing pressure $p_n(z)$—namely $R(z)$, $r_{eff}(z)$, $t_{eff}(z)$— are evaluated at the end of each axisymmetric stage. In this way, the method produces distinct profiles which are transferred to the corresponding plane-strain stages.*

Specifically, the open-roof configuration is represented by progressively suppressing the confinement correction above the open-crown elevation—taken to decrease linearly to zero at the ground surface for that stage—while the extracted confinement profile is retained unchanged over the embedded, ring-closed portion of the chamber.
At each stage, boundary hoop stress $\sigma_\theta(R,z)$ is extracted, and the perturbation $\Delta\sigma_\theta(R,z) = \sigma_\theta(R,z) - \sigma_{\theta,\infty}(z)$ is calculated, with $\sigma_{\theta,\infty}(z) \approx k_0\sigma_v(z)$.

Outward from the boundary, the effective radius $\boldsymbol{r_{eff,n}}$is identified by applying:

$$\kappa_{sel} = \frac{\Delta\sigma_\theta(r_{eff,n},z)}{\Delta\sigma_\theta(R,z)} \quad (10)$$

From this, the numerical confinement thickness and normalized width are computed:

$$t_{eff,n}(z) = r_{eff,n} - R(z), \beta_n(z) = \frac{t_{eff,n}(z)}{R(z)} \quad (11)$$

The numerical depth profiles of the cavity radius R(z), the confinement thickness t_eff(z), and the effective radius r_eff(z), computed from the axisymmetric reference analysis, are presented as depth-dependent profiles. These parameters control the spatial extent of the confinement zone around the cavity and form the basis for computing the equivalent stabilizing pressure.

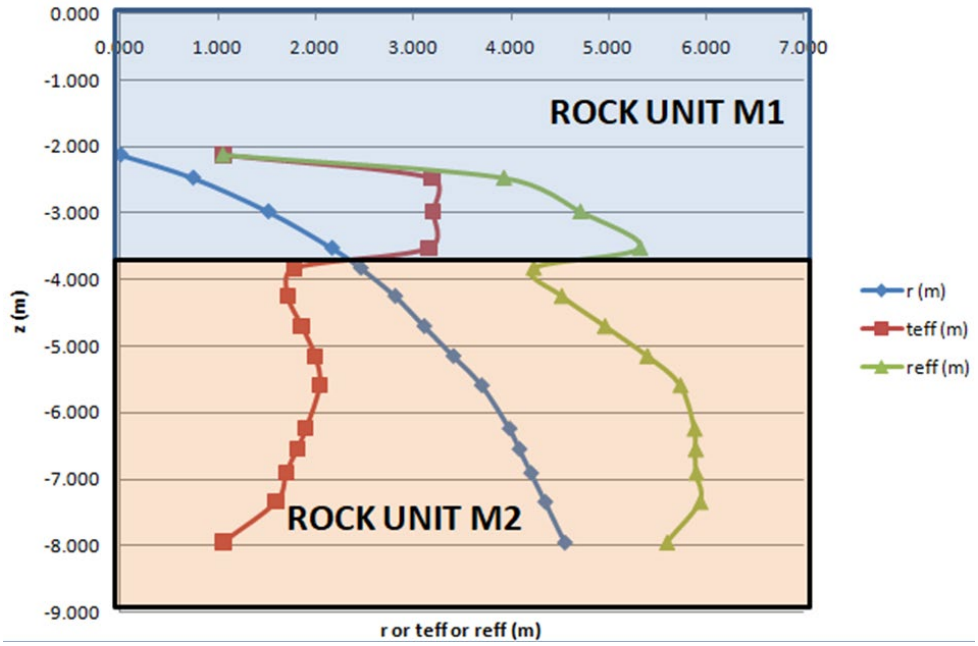

Figure 5. *Numerical depth variation of cavity radius $r(z)$, confinement thickness $t_{eff}(z)$, and effective confinement radius $r_{eff}(z)$, as extracted from the axisymmetric model for the initial excavation stage. The two primary rock units (M1 and M2) are indicated.*

Comparison of analytical and numerical confinement functions

Figure 6 compares the stabilizing pressure profile $p_n(z)$obtained from the Kirsch-type analytical formulation (using $\sigma_\theta(R,z)$) derived both analytically and numerically) with the corresponding profile derived from the staged axisymmetric numerical analysis. In the lower rock unit (Rock Unit M2), the two curves exhibit a similar depth-dependent trend, indicating that the analytical formulation captures the overall evolution of circumferential confinement with depth.
Systematic differences are nevertheless observed in terms of magnitude. In the upper rock unit (Rock Unit M1), the axisymmetric numerical analysis predicts higher confinement levels than the analytical solution, reflecting the influence of idealized geometry in the analytical formulation, as well as stratigraphy and material heterogeneity. In contrast, within the lower unit (Rock Unit M2), the analytical solution tends to slightly overestimate confinement relative to the numerical model. *In the present application, this staged dependence is retained explicitly by extracting and transferring* $\mathrm{p_n^j(z)}$ *at each discrete axisymmetric stage.*
These discrepancies are attributed to geometrical effects (ideal conoidal shape for the analytical calculations) and geological effects, including material contrasts and stratification, which cannot be

represented by the homogeneous elastic assumptions underlying the Kirsch-type solution. The comparison therefore highlights the need for calibration of the analytical confinement function against the axisymmetric numerical response prior to its transfer to asymmetric plane-strain models.
Differences between the Kirsch-type analytical estimate and the numerical reference are expected because the analytical solution represents an instantaneous elastic excavation in an idealized stress field and geometry, whereas the numerical approach follows the staged stress path of the monument (geostatic initialization → excavation → cover degradation/weathering → roof loss) in a stratified medium. In the present methodology, analytical confinement profiles may nevertheless be computed for each discrete stage (closed-roof excavation, weathered cover, and open-roof configuration) by updating the stage geometry and far-field reference stresses; however, these analytical stage profiles do not retain stress history and therefore cannot reproduce path-dependent redistribution effects. Consequently, the redistribution history can influence the extracted boundary hoop stress $\sigma_\theta(R,z)$ and the inferred confinement extent—particularly in the upper unit where weathering and property contrasts are stronger—so the axisymmetric results provide the stage-resolved reference $\mathrm{p_n^j(z)}$ used to calibrate κ factor and refine the analytical estimates prior to transfer to the corresponding asymmetric plane-strain stages. Where axisymmetric modelling is not feasible, the stage-wise analytical profiles can still be used as a conservative preliminary substitute, with sensitivity to κ reported to bound uncertainty.

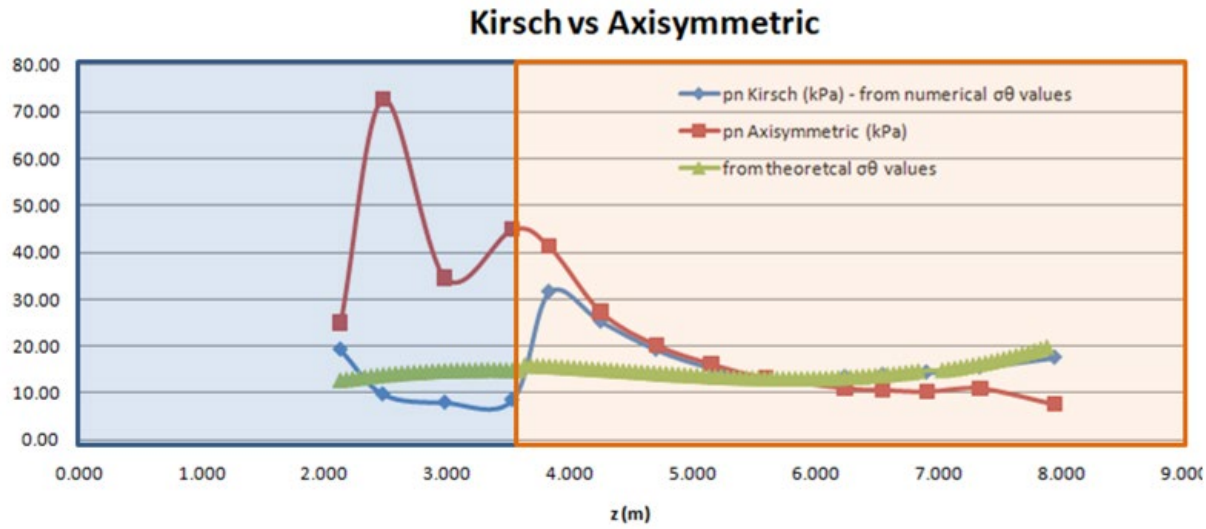

Figure 6. *Comparison of the stabilizing pressure profile $p_n(z)$ derived from the Kirsch-type analytical expression and from the axisymmetric numerical model (initial excavation stage).*

Corrected asymmetric analyses and stability mechanisms

The site-scale model is analyzed using plane strain models that incorporate the actual site asymmetry, including stratigraphy, discontinuity anisotropy where applicable, slope effects, and shelter-induced surface loads. Two modelling configurations are examined: (i) an uncorrected plane-strain model, in which no circumferential confinement is introduced, and (ii) a corrected plane-strain model, in which the depth-dependent confinement function $p_n(z)$ is applied in a staged manner, using either analytically or numerically derived values.

A direct comparison between the resulting displacement fields clearly illustrates the mechanical role of the transferred circumferential confinement. In the conventional plane-strain model (section with the most adverse orientation for the critical joint) without confinement correction, large and spatially extended horizontal displacements develop around the cavity under geostatic loading, indicating a global tendency of the rock mass to deform toward the excavation void (Figure 7).

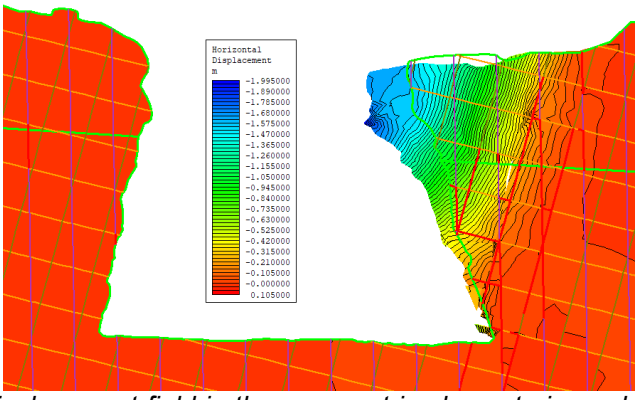

Figure 7. *Horizontal displacement field in the asymmetric plane-strain model without application of the circumferential confinement correction (failure of the right slope, T1 tomb).*

For the same loading conditions, the introduction of the stabilizing pressure derived from the axisymmetric confinement analysis leads to a fundamentally different response. Horizontal displacements are drastically reduced and become strongly localized in the immediate vicinity of the cavity boundary, while the surrounding rock mass remains comparatively stable. This effect is evident in Figure 8 (left), which represents the current geostatic condition with confinement correction applied. The same stabilizing effect is observed under seismic loading corresponding to the major historic earthquake of 464 BC (M = 6.8), with the associated pseudostatic coefficients applied as indicated in the figures. As shown in Figure 8 (right), the cavity remains stable even under this adverse seismic scenario, confirming that the confinement-transfer procedure restores the dominant stabilizing mechanism that is otherwise suppressed in conventional plane-strain analyses.

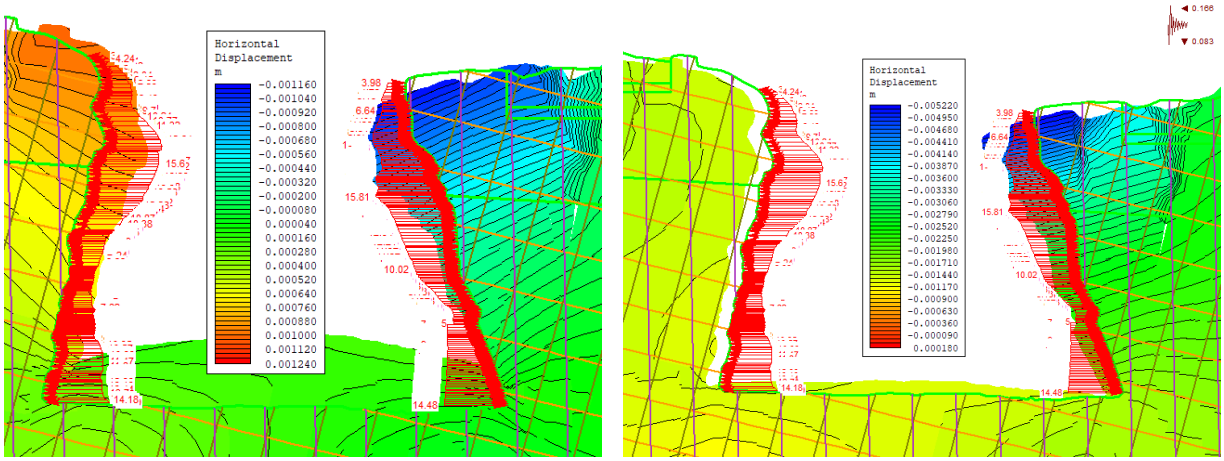

Figure 8. *Left: Horizontal displacement field in the asymmetric plane-strain model with applied confinement correction under current geostatic conditions (T1 tomb – present state). Right: Corresponding displacement field under a major historic seismic event (464 BC, M = 6.8), showing preserved stability due to circumferential confinement (numerically derived stabilizing pressures).*

Figure 9 complements Figure 8 by repeating the current geostatic and pseudostatic seismic scenarios using the confinement correction derived from the stage-wise Kirsch formulation, rather than from the staged axisymmetric extraction. The overall displacement patterns remain consistent, supporting the practical applicability of the analytical estimate as a rapid proxy when axisymmetric reference modelling is not available. The marginal seismic response observed in Figure 9 (right) is attributed to differences between the analytical and numerically extracted confinement profiles inherited from the preceding excavation and degradation stages (see also Figure 6): the analytical solution represents an instantaneous elastic response in an idealized stress field and geometry, whereas the axisymmetric model follows the staged stress path in a stratified medium. For final design checks, the preferred procedure is therefore to transfer the stage-resolved $p_n^j(z)$ *profile extracted from the corresponding axisymmetric stage; the analytical stage profiles provide a conservative screening alternative and an independent consistency check.*

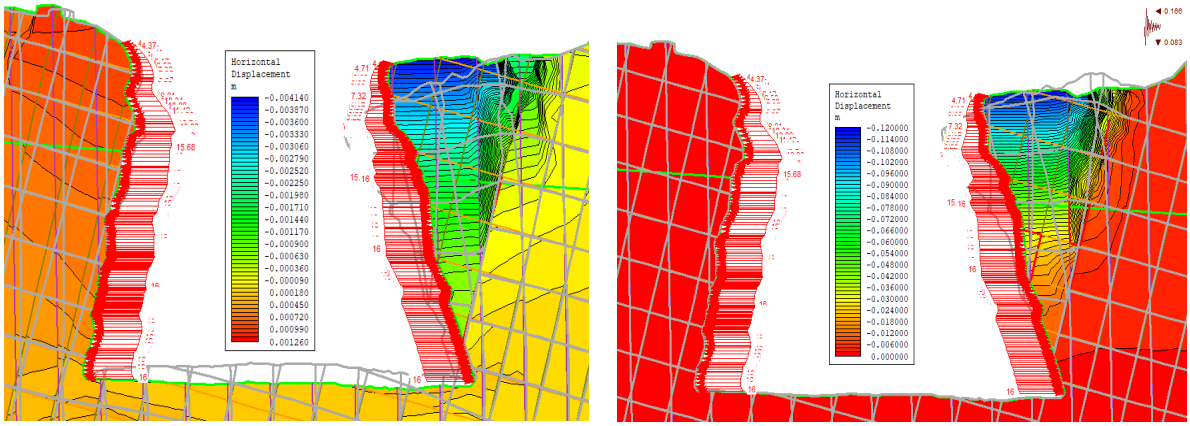

Figure 9. *Left: Horizontal displacement field in the asymmetric plane-strain model with applied confinement correction under current geostatic conditions (T1 tomb – present state). Right: Corresponding displacement field under a major historic seismic event (464 BC, M = 6.8),* indicating *preserved stability due to circumferential confinement (theoretically derived stabilizing pressures (Kirsch equations).*

Design of intervention measures

To protect the Tomb Complex at Pellana from environmental exposure, including the open-roofed Tomb 1, a large protective shelter is planned (Orestidis G., 2022). Numerical analyses indicate that the additional loads associated with the shelter may induce localized overstressing and potential instability in the upper cavity ring zone (Material Zone M1). For this reason, targeted stabilization measures are required to ensure the structural integrity and long-term preservation of the monument.

The proposed interventions (Egglezos, 2023) are directly related to the shelter works and are intended to be implemented before construction begins. The stabilization scheme consists of three circumferential rows of fully bonded rock anchors (Figure 10, left), each with a length $L = 6.0$ m. The anchors comprise 18 mm diameter stainless-steel bars (AISI 316LN 500) installed in 46 mm diameter boreholes and subsequently pressure-grouted using a white-cement-based grout. The anchors are arranged in a regular 1.0×1.0 m grid in plan (Figure 10, right), providing distributed reinforcement of the upper cavity zone.

Figure 10. *Arrangement of proposed measures for Tomb T1. Transverse Section S-18 (left) and Plan view of Tomb T1 (right). Excerpt from the Drawings of Structural Study (Egglezos, 2023).*

CONCLUSIONS

This paper has presented a simplified pseudo-3D methodology for the stability assessment of ring-type carved chambers under asymmetric geological and loading conditions. The approach is based on the recognition that circumferential (hoop) confinement is an inherently three-dimensional stabilizing

mechanism: it is captured in axisymmetric analysis but is suppressed in plane-strain modelling, even though plane strain is often essential for representing realistic stratigraphic and boundary-condition asymmetry. To overcome this limitation, the stabilizing contribution of hoop confinement is reintroduced into the plane-strain model through a staged, depth-dependent equivalent confinement pressure $\mathrm{p_n^j(z)}$*, (with j, denoting the relevant stage) thereby restoring the missing mechanism in a controlled and transparent manner while preserving the capability of 2D analysis to represent site-specific asymmetry.*

A clear definition of the confinement decay parameter κ *(adopted as the remaining fraction of the excavation-induced hoop-stress increment) leads to closed-form analytical expressions under a Kirsch-type decay assumption. In this framework, the normalized effective confinement width is* $\beta(z) = 1/\sqrt{\kappa} - 1$*, and the equivalent stabilizing pressure follows* $\mathrm{p_n^j(z)} = \Delta\sigma_\theta^j(R,\mathrm{z}) \cdot (1-\kappa)$*, providing an explicit analytical link between hoop-stress redistribution and the confinement to be reintroduced into plane strain. Importantly, analytical profiles can be computed for each discrete stage (closed-roof excavation, cover degradation/weathering, and roof loss/open roof) by updating geometry and far-field reference stresses; however, they represent instantaneous elastic responses and do not retain the stress path history.*

The axisymmetric analyses provide the stage-resolved reference against which analytical parameters are calibrated: a distinct confinement profile $\mathrm{p_n^j(z)}$ *is extracted from each axisymmetric stage and transferred to the corresponding plane-strain stage, preserving the staged stress path of the monument. In this sense, the analytical formulation plays a complementary role: it offers a rapid stage-wise estimate and an independent consistency check, while the axisymmetric results—when available—enable calibration of* κ *and refinement of the confinement profiles prior to transfer. Where axisymmetric modelling is not feasible, the analytical stage-wise profiles may still be used as a conservative preliminary substitute, supported by sensitivity to* κ*.*

The far-field reference state for hoop stress may be defined using the at-rest horizontal stress concept, $\sigma_{\theta,\infty}(z) = K_0 \cdot \gamma \cdot z$*, with* K_0 *selected as a constant or from generalized correlations (Pantelidis, 2019). Application to the Pellana Tomb 1 framework demonstrates how stage-wise confinement transfer improves the interpretation of stability mechanisms and supports more proportionate, conservation-compatible intervention design by distinguishing physical instability mechanisms -controlled by geology, geometry, and surface loading- from artefacts associated with plane-strain suppression of hoop confinement. Overall, the proposed framework supports more rational, transparent, and conservation-compatible engineering decisions for carved rock monuments.*

ACKNOWLEDGEMENTS

The authors wish to express their gratitude to Mr Manolis Tzannidakis, Civil Engineer (MSc), for his valuable support during the preparation of this scientific communication. In particular, they gratefully acknowledge his assistance with the development of the illustrative material and the careful formatting of the manuscript. They also thank him for his contribution to the preparation of the underlying study, which provided the basis for the present work.

REFERENCES

Egglezos, D. (2023). Structural study for the restoration and promotion of the Mycenaean cemetery Pellana, M. Sparta, R. Laconia. Ephorate of Antiquities of Laconia.

GEO.PER. S.A. (2022). Geotechnical study for the restoration and promotion of the Mycenaean cemetery Pellana, M. Sparta, R. Laconia. Ephorate of Antiquities of Laconia.

Hoek, E., & Brown, E. T. (1980). Underground excavations in rock. Institution of Mining and Metallurgy, London.

Hoek, E., Carranza-Torres, C., & Corkum, B. (2002). Hoek–Brown failure criterion—2002 edition. Proceedings of the North American Rock Mechanics Symposium, Toronto.

Kirsch, G. (1898). Die Theorie der Elastizität und die Bedürfnisse der Festigkeitslehre. Zeitschrift des Vereins Deutscher Ingenieure, 42, 797–807.

Kramer, S. L. (1996). Geotechnical earthquake engineering. Prentice Hall.

Orestidis, D. (2022). Photogrammetric survey of the Mycenaean tombs, M. Sparta, R. Laconia. Ephorate of Antiquities of Laconia.

Orestidis, G. (2022). Architectural study for the restoration and promotion of the Mycenaean cemetery Pellana, M. Sparta, R. Laconia. Ephorate of Antiquities of Laconia.

Pantelidis, L. (2019). The generalized coefficients of earth pressure: A unified approach. Applied Sciences, 9(24), 5291.

Rocscience Inc. (2023). RS2 – 2D finite element analysis for excavations in rock and soil, user's guide. Toronto, Canada.

Seed, H. B., & Whitman, R. V. (1970). Design of earth retaining structures for dynamic loads. In Proceedings of the ASCE Specialty Conference on Lateral Stresses in the Ground and Design of Earth Retaining Structures, Cornell University.

Timoshenko, S. P., & Goodier, J. N. (1970). Theory of elasticity (3rd ed.). McGraw-Hill.